# Integration of Novel mm-wave Components on Flexible Organic Substrates for Automotive Radar Applications

Amin Rida [1], Farzad Nasri [1], Alexandros Margomenos [2], and Manos M. Tentzeris [1]

[1]*GEDC/School of ECE, Georgia Institute of Technology, Atlanta, GA, 30332-250, USA*

[2]*Toyota Research Institute North America, Ann Arbor, MI, 48105, USA*

arida@ece.gatech.edu

***Abstract*—This paper reports on novel mm-wave passive components; namely vertical broadband transitions, a high efficiency aperture coupled microstrip antenna array, and their integration on flexible and organic Liquid Crystal Polymer (LCP) to realize a simple, low cost, passive front end module using a system on package (SOP) concept. Coplanar Waveguide-Coplanar Waveguide-Microstrip (CPW-CPW-MSTRIP) and CPW-CPW-CPW 3D transition designs using strategically placed vias and tapering of the CPW ground planes, which suppress radiation loss and optimize the performance over a very broad frequency range are presented. A four-element aperture coupled microstrip antenna array with a high efficiency of 82% and a gain of 12dBi at 77GHz is reported. These structures are simple to realize and are compatible with low-cost substrate fabrication guidelines, thereby allowing for the easy feeding of embedded IC's in 3D modules, especially in compact automotive radar applications and beam-steering wideband antenna arrays. Measurement results are provided for the 3D transitions to show the proof of concept for the front end passive system.**

## I. INTRODUCTION

The demand for inexpensive, low-profile, reliable, and low-power consumption radar systems is driven by today's need for intelligent automobiles. Radar systems have become a standard in automotive safety due to the low performance of alternative solutions, especially in severe weather conditions. Today's automobiles implement a combination of short-range radar (SRR) operating at 24 GHz, long-range radar (LRR) operating at 77 GHz, and video-based scanning systems in order to provide automated safety control through collision mitigation or avoidance, smart cruise control, parking aids, blind spot surveillance, and road awareness. However, current implementations are costly, bulky, and do not provide a sizeable angular resolution. This is primarily due to the current use of very expensive substrates (e.g. Si, GaAs, and Alumina) and due to the specialized fabrication process required, such as micromachining of waveguides which are used in current systems, which result in bulky and narrowband overall mm-wave systems [1].

In order to achieve high gain and directive radiation with the aforementioned constraints, this paper proposes the design and integration of a 3D vertical transition used to connect a mm-wave antenna array constructed on a Liquid Crystal Polymer (LCP) substrate with a Silicon Germanium chip (packaged flip-chip mounted T/R module). In order for the radar to function properly, the 3D vertical transition needs to be wideband, small in size, low-cost, and compatible with commercially available LCP design rules. In addition, the transition must have low insertion loss and low return loss.

The radar system implements a mm-wave antenna array that provides a larger antenna aperture, thereby yielding a proportionally larger gain by focusing radiation in the direction of propagation. The array is constructed on a LCP substrate, which is a low-cost dielectric material with several promising properties. LCP has a low and stable water absorption rate that is less than 0.04% and a nearly constant dielectric constant of 3.1. In addition, LCP has a very low loss tangent of only 0.002, which increases to only 0.0045 at 110 GHz, thereby making LCP very suitable for mm-wave applications [2].

A variety of antennas can be used in mm-wave radar systems, including but not limited to cassegrain antennas and lens antennas. However, such antennas are too large for low-profile automobile applications. As a result, this paper discusses the implementation of an aperture coupled mm-wave antenna array with slot feeding. This design allows for the use of slots to couple the microstrip feed line to each patch antenna element. The slots or apertures are located on the ground plane, thereby permitting coupling between the top and bottom substrates. With the appropriate optimization of the dimensions and positioning of array elements, a sizeable gain, high bandwidth and radiation efficiency can be achieved.

While this paper discusses the design and integration of a four-element array, it is easy to see that the gains required for an automotive radar antenna system can be achieved by simply cascading additional elements in a phased array configuration. In the future, the use of similar low-profile and cost-effective systems can provide automobiles with improved safety mechanisms, including but not limited to automated driving and seamlessly integrated radar-based communication between vehicles for improved road coverage.

## II. Wideband 3D Transitions

Previous work in high frequency transitions have mainly looked at waveguide-to-microstrip [3], wideband Si micromachined transitions [4] and mm-wave transitions yet only characterized up to 60 GHz [5]. This section presents the design of the 3D vertical transition that connects the antenna array with the T/R module. This is illustrated in Fig. 1 below.

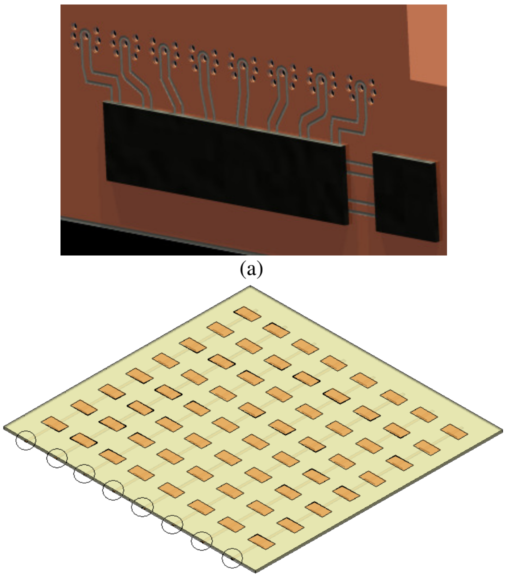

(a)

(b)

Fig. 1. mm-wave System Concept (a) Bottom view of transition to chip connection and (b) top view of transition to array connection with the circles

The design consists of one via-based vertical transition from center to center conductors, that is used to connect the transmission lines printed on both sides of a single LCP layer ($\varepsilon_r$ of 3.16 and thickness of 4 mils), as well as grounding vias connecting the top and bottom ground layers. Shown in Fig.2 is the schematic of the design with the specific via placements. The bottom layer (Fig. 2b) starts as a CPW launch with characteristic impedance 50 Ohms, realized appropriately by choosing the signal line width and the gap between the signal line and the ground. The CPW slot width (~85 um) is responsible for maintaining a desired CPW mode for the wide frequency throughout the CPW section of the transmission line (top and bottom), which is kept at a constant value around the via pad, resulting in minimum field reflections and very good impedance matching.

The transition via lies within a wide circular disk shape to accommodate for the via pad with dimensions specified by fabrication specifications for the via metallization. The specific dimensions of the transition via as well as the via pad that surrounds it were chosen in accordance with the RF design requirements as well as the fabrication design guidelines and tolerances.

The CPW ground planes on the top layer have been tapered at an angle α of ~27 degrees with a ground width of 4.25 x the microstrip signal line width as shown in Fig. 2a. In addition, vias with a radius of 3 mils have been strategically placed around the transition and the ground plane edges in order to achieve the optimum broadband RF performance. This is achieved by minimizing the return loss (RL) and insertion loss (IL) due to impedance mismatches and by eliminating the radiation loss due to the open-end effects.

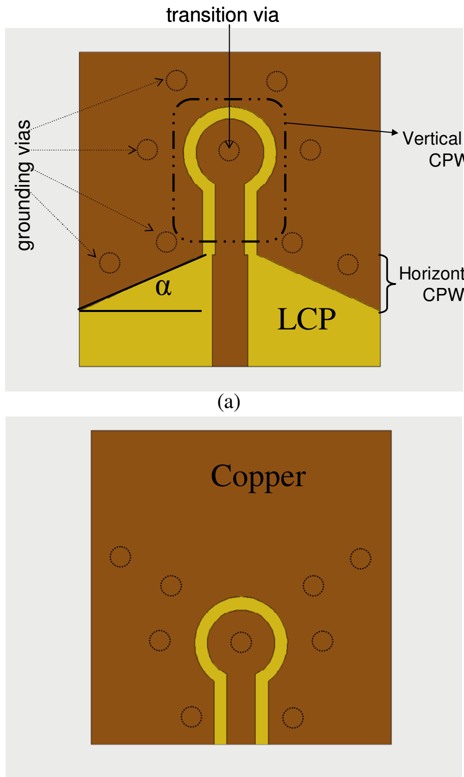


(a)

(b)

Fig. 2. Wideband Vertical CPW-CPW-MSTRIP Transition (a) top view and (b) bottom view

The measured and simulated S-parameters for the CPW-CPW-MSTRIP transition are plotted in Fig. 3 demonstrating a wideband operation from 60 to 100 GHz shown by the -10 dB bandwidth. It has to be noted that both RL and IL were affected considerably due to fabrication and measurement setup issues. In the fabricated structures, it was observed that metal over-etching has occurred for both CPW and microstrip metal lines; also, the vertical vias have been misplaced off-center within the pad; both issues have been studied in further detail using a sensitivity analysis explaining the experimental shift of the minimum points on the RL plot. The over-etching is very critical for mm-wave frequency, especially in the CPW RF launches as well as in the width of the MicroStrip line, so it is expected to be the main factor of the difference in RL and IL levels. In order to minimize the effect of the metal chuck, the measurement setup, used an LCP layer of 16 mils thickness surrounding the fabricated structures, which in turn was placed on a glass platform. This multidielectric configuration changed the effective dielectric constant of the transition substrate realizing a “superstrate” for the transmission lines in the lower side; another issue significantly affecting the measurements. Thus, it is another significant factor responsible for the difference in periodicity in RL plot as shown in Fig. 3. The measured insertion loss is -3.7 dB at 76.5 GHz for the back-to-back transition which translates to -1.6 dB for a single transition as illustrated in Fig.2. The simulated E-field from HFSS is presented demonstrating that all the fields are confined along the signal line, with minimal radiation due to the open-end effects.

Fig. 4 presents the measured and simulated response of the CPW-CPW-CPW transition; a similar 3D transition as the one described above but terminated with a CPW line. A -10 dB S11 bandwidth covers the whole frequency range from 60-100GHz and the measured insertion loss is -2.9 dB at 76.5 GHz for the back-to-back transition which translates to -1.3 dB for a single transition. All dimensions on the designed structures are based on existing, commercially available design rules and the use of mechanical drilling for via formation.

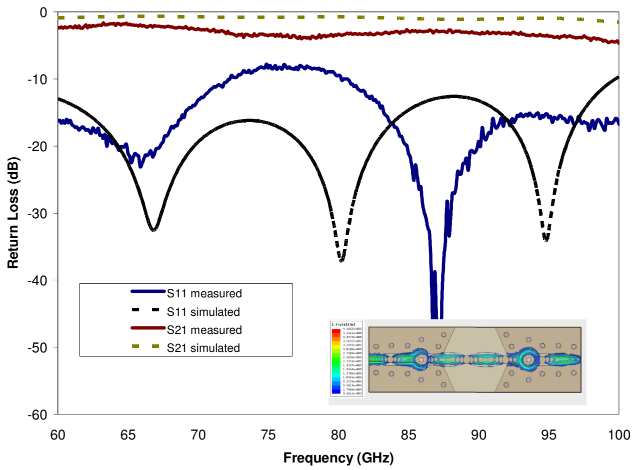


Fig. 3 S-Parameters for 3D Transition CPW-CPW-MSLINE

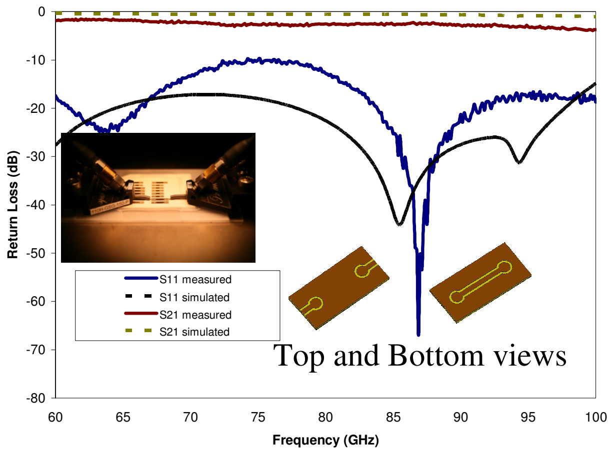


Fig. 4 S-Parameters for 3D Transition CPW-CPW-CPW and photo of measurement setup

## III. ANTENNA ARRAY

A variety of antennas can be used in millimetre-wave radar systems. However, the design of an automotive radar system requires a cost-effective and compact approach in order to provide the seamless integration of affordable and efficient collision avoidance systems in today's automobiles. In order to achieve a cost-effective and compact antenna design, a slot feed patch antenna is used in this effort.

The slot feed patch antenna array implements four elements on a 4 mil thick LCP substrate in order to achieve a sizeable gain for long range automotive radar applications. The four elements were optimized around a $\lambda_0$ / 2 separation between the first element and the point of integration where $\lambda_0$ is the free space wavelength at 77 GHz. Fig. 5 shows a schematic of the optimized four element antenna array.

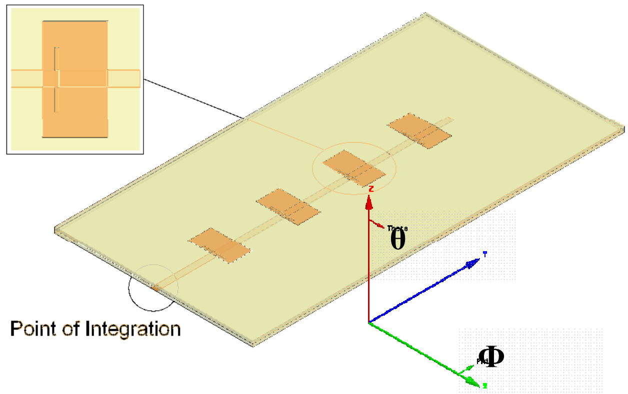


Fig. 5 Schematic of the four element antenna array.

In order to minimize the return loss and produce a sizeable gain, the dimensions and spacing of the patches and slots were optimized. It was found that a patch width of approximately 1.5 mm and patch length of 0.835 mm along with a slot width of 820 µm and slot length of 50 µm yielded the optimum return loss, gain, and radiation efficiency.

The return loss for the array is shown in Fig. 5 below.

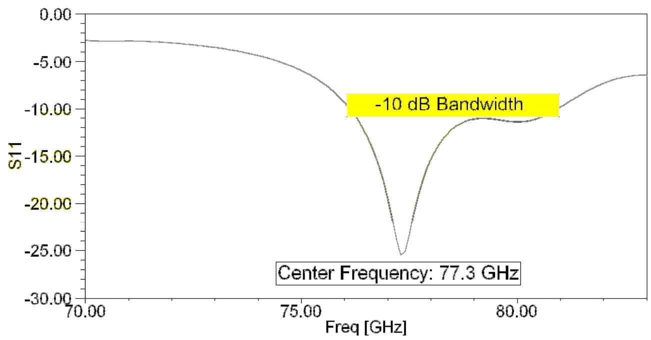


Fig. 5 Return loss of the four element antenna array shown in fig. 4(a)

Simulation results show a -10 dB bandwidth of approximately **6.3%** and a center frequency of 77.3 GHz.

The performance of the optimized array was further verified by inspecting the radiation pattern shown in Fig. 6. The radiation pattern shows a high directivity while maintaining both minimized and symmetric side lobes. A front-to-back ratio of 17.76 dB and a front-to-side ratio of 17.98 dB were achieved. The front-to-back ratio was measured between the main lobe and the strongest back lobe. The front-to-side ratio was measured between the main lobe and the strongest side lobe. In addition, the results yielded a radiation efficiency of approximately 82% and a maximum gain of approximately 12.34 dB. Several variations of the array yielded slightly higher maximum gains at the expense of larger side lobes. As a result, the optimized design with the aforementioned gain was chosen.

The optimized design resulted in a maximum gain of 12.34 dB with only four elements. Therefore, it is easy to see that the gains required for an automotive radar antenna system can be achieved by simply cascading additional elements in a phased array configuration.

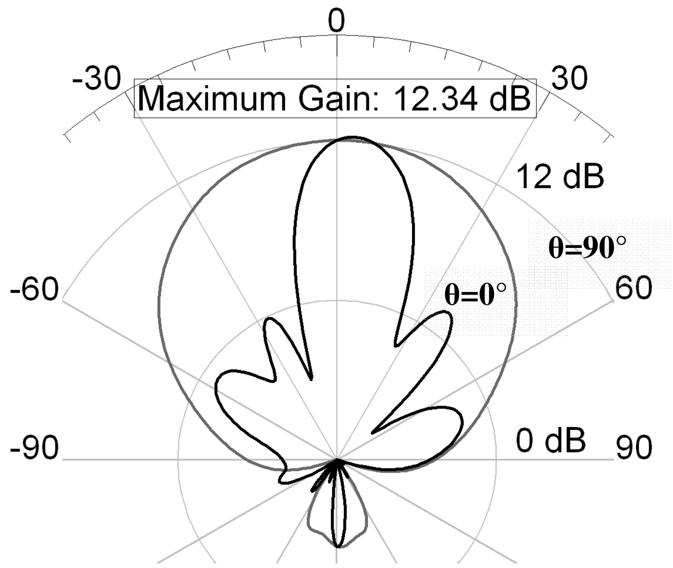


Fig. 6 Radiation pattern of the four element antenna array.

## IV. Integration and Future Work

Current work of this project constitutes the integration of the two above sections: 3D transition and the antenna array. In addition, further development of the large antenna array (Fig. 1.b) is underway as well. Another issue that mm-wave frequencies suffer is the increase of the loss upon bending passive structures such as transmission lines, which in turn deteriorates the overall mm-wave system. The current work has designed and characterized wideband and low-loss bends for CPW and microstrip lines that will be used in the T/R feeds and the antenna array respectively.

## V. Conclusions

This paper presented two successful 3D transitions and the design of a 4-element microstrip slot fed antenna array with good efficiency and a 6% bandwidth for mm-wave automotive radar applications. An overview of each design section of this mm-wave module: 3D transition, antenna array, cross talk reduction mechanisms, CPW and microstrip transmission line bends, as well as their integration will be discussed at the conference with characterization results and remarks about design and measurement phases.

## References

[1] M. Schneider, “Automotive Radar – Status and Trends”, Proc. German Microwave Conference GeMiC, pp. 144-147, Ulm, Germany, April 2005

[2] D. C. Thompson, O. Tantot, H. Jallageas, G. E. Ponchak, M. M. Tentzeris, and J. Papapolymerou, "Characterization of liquid crystal polymer (LCP) material and transmission lines on LCP substrates from 30-110 GHz," *IEEE Trans. Microwave Theory Tech*., vol. 52, no.4, pp. 1343-1352, April 2004.

[3] Y. Deguchi, K. Sakakibara, N. Kikuma, H. Hirayama, Design and optimization of mm-wave microstrip-to-waveguide transition operating over broad frequency bandwidth, IEICE Transactions on Electronics, vol. E90-C, no.1, pp. 157-164, January 2007.

[4] A. Margomenos, Y. Lee, L.P.B. Katehi, “Wideband Si Micromachined Transitions for RF Wafer-Scale Packages”, IEEE Topical Meeting on Silicon RF Components SiRF2007, Long Beach, CA, January 2007.

[5] A. Stark, A.F. Jacob, “A Broadband Vertical Transition for Millimeter-Wave Applications”, European Microwave Conference 2008 Digest, pp. 476-479, October 2008, Amsterdam, NETHERLANDS.